Fuel 260 (2020) 116308

SCALING SPRAY PENETRATION AT SUPERSONIC CONDITIONS THROUGH SHOCKWAVE ANALYSIS

Salvador, Francisco Javier[1] (*), De la Morena, Joaquín [1], Taghavifar, Hadi [2], Nemati, Arash. [3]

[1] CMT-Motores Térmicos, Universitat Politècnica de València

Camino de Vera s/n, E-46022, Valencia, Spain.

[2] *Department of Mechanical Engineering, Faculty of Engineering, Malayer University, Malayer, Iran*

[3] *Faculty of Mechanical Engineering, University of Tabriz, 29th Bahman Blvd., Tabriz, Iran*

(*) Corresponding author:

Dr. F. Javier Salvador, fsalvado@mot.upv.es

CMT-Motores Térmicos, Universitat Politècnica de València

Camino de Vera s/n, E-46022, Valencia, Spain.

Telephone: +34-963879659

FAX: +34-963877659

Keywords

Diesel spray, shockwave, penetration, visualization

Abstract

In the current paper, an investigation of the supersonic flow effect on shockwave generation and diesel spray penetration scaling has been performed. For this purpose, spray visualization tests have been carried out in a constant-pressure chamber at room temperature using shadowgraphy technique. Two working gases have been used: nitrogen, with similar thermodynamic characteristics to the engine environment, and sulfur hexafluoride, aimed at producing supersonic conditions at moderate injection pressure values. A total of 60 operating points, including different nozzle geometries, injection pressures and chamber densities have been studied. From the visualization study, two different kinds of shockwaves have been detected: normal or frontal, for moderate spray tip Mach (between 1 and 1.5); and oblique, when the Mach is higher than 1.5. The penetration results show that, for the same injection conditions in terms of injection pressure and chamber density, the spray propagation is equal for SF_6 and N_2 when the spray is on subsonic conditions, while penetration is higher for SF_6 when supersonic velocity is reached. This behavior has been related to the density gradient appearing across the shockwave. A new methodology to extrapolate supersonic penetration from the well-known subsonic penetration law has been proposed, showing good agreement with the experimental results.

1. Introduction

Spray penetration is one of the key physical parameters involved in diesel combustion process. Traditionally, spray penetration has been linked to the nozzle outlet momentum (which depends on the injection pressure) and the density ratio between the fuel and the gas inside the combustion chamber, with an exponent around -0.25 [1–3]. Furthermore, several authors have noticed that the dependency of this spray penetration shows two different trends: initially, penetration increases linearly with time, while later on the spray tip velocity reduces, resulting in a square root scaling of penetration versus time [4,5]. This transition time has been correlated with the transient behavior of the momentum at the outlet of the nozzle due to the injector needle dynamics [6].

In the recent years, fuel injection systems design has evolved towards higher injection pressures. On the one hand, higher turbulence levels at the nozzle outlet help to improve spray atomization and air entrainment [7–10]. On the other hand, faster spray penetration can help to achieve better air utilization and improve combustion speed at high loads [11]. Linked to this injection pressure increase, several researchers have noticed that the spray tip can reach supersonic conditions. Kostas et al. [12] realized that supersonic conditions during the initial spray stages could affect spray penetration due to compressibility effects. Hillamo et al. [13] used backlighting visualization to detect shockwaves formation attached to the spray edge. Jia et al. [14] made experiments at ultra-high pressure (400 MPa) and showed that two kinds of shockwaves can appear: spherical (or bow) and oblique. In a subsequent study, Jia et al. [15] compared the spray penetration at this supersonic conditions with the well-established spray penetration correlations, concluding that spray propagation was affected by the supersonic regime. Wang et al. [16] made a similar investigation, where also spray cone angle and atomization (in terms of Sauter Mean Diameter) began to vary when supersonic conditions were reached. Finally, Song et al. [17] studied the shockwave angles and the implications on air entrainment. Nevertheless, in any of the aforementioned investigations an analysis aimed at providing an analytical expression to estimate the supersonic spray penetration law has been performed.

In the current paper, a further investigation on supersonic spray propagation characteristics is made. For this purpose, fuel is injected on a pressurized sulfur hexafluoride (SF_6) environment, aimed at reaching very high local Mach numbers with a standard fuel injection system hardware. Spray and shockwave visualization is made using shadowgraphy technique on a constant pressure vessel. The results from visualization on SF_6 are compared with results made on nitrogen atmosphere, where the chamber pressure has been adapted in order to achieve the same gas density but on subsonic regime. Later on, a methodology to estimate the supersonic spray penetration from the subsonic conditions data is proposed and validated, which is the main contribution from the current work.

As far as the paper structure is concerned, five sections are developed. Section 2 summarizes the main aspects of the experimental setup and used methodology. Section 3 analyzes the shockwave visualization results. The methodology for spray penetration evaluation at supersonic conditions is proposed and evaluated in Section 4. Finally, the main conclusions extracted from the study are drawn in Section 5.

2. Experimental setup

Liquid spray penetration is characterized on a constant pressure chamber at room temperature conditions (25ºC) [18]. A picture of this spray visualization chamber can be seen in Figure 1. The vessel has three rectangular optical accesses allowing to perform different optical diagnostics for spray characterization purposes. Initially, the chamber is filled with nitrogen, reproducing engine-like density conditions in a non-reactive environment. In particular, four levels of chamber pressure (1, 2, 3 and 4 MPa) are tested, corresponding to density values of 11.3, 22.6, 33.9 and 45.2 kg/m^3. Later on, the same density conditions are reproduced using sulfur hexafluoride (SF_6). The main advantage of this gas consists of its higher molecular weight (146.06 g/mol vs. 28.014 g/mol for nitrogen) and lower speed of sound (136.5 m/s vs. 351.8 m/s for nitrogen at room conditions). Thus, allowing local Mach in the spray tip is achieved at moderate injection pressures. To achieve the same densities, chamber pressures of 0.19, 0.38, 0.57 and 0.76 MPa are selected for SF_6.

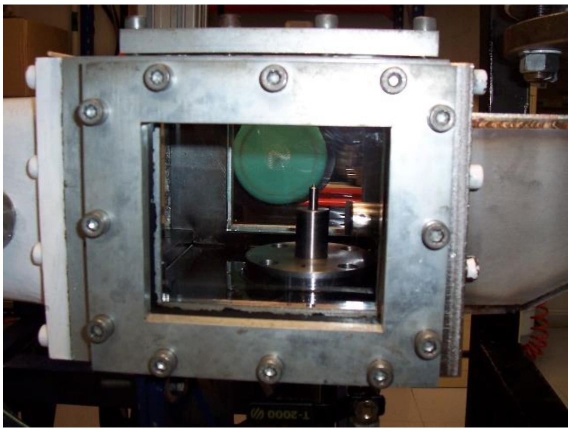

Figure 1. Detail of spray visualization test rig.

A Bosch common-rail fuel injection system capable of reaching up to 160 MPa pressure is used for the experiments. The solenoid injector is equipped with five different single-hole axi-symmetric nozzles, with outlet diameters ranging from 0.119 to 0.206 mm. For each nozzle and density condition, three levels of injection pressure are evaluated (50, 80 and 130 MPa) in order to reach both subsonic and supersonic conditions for the spray penetration evaluation. Thus, a total of 60 tests are performed for each filling gas. All tests have been performed using a European standard winter diesel fuel as working fluid. The main physical properties of this fuel, including density and viscosity, are reported in [19].

It has to be noted that the reduction in the discharge pressure achieved for the SF_6 tests could induce severe changes in the spray propagation characteristics if cavitation was induced inside the nozzles. However, for the set of nozzles used in the study (which are convergent) a previous hydraulic characterization shows that no cavitation appears for the working pressures used in the study.

Regarding the optical setup, single-pass shadowgraphy technique is used to visualize both the spray and the shockwaves evolution. This technique is based on illuminating from one side of the spray with a Xe-arc lamp, and capturing the light with a camera on the opposite side. When there is a density change across the optical path (either produced by the spray droplets or by the shockwave), light beams deviate due to the different refractive index, producing a shadow on the camera sensor [20,21]. For this particular arrangement, a Photron high-speed camera set up at 40000 frames per second is employed. Each conditions is repeated a total of 8 times in order to evaluate the test repeatability. An example of the images obtained on the SF_6 tests, including the spray and the related shockwave, is seen in Figure 2. This images corresponds to an injection pressure of 80 MPa, a gas density of 22.6 kg/m^3 and an elapsed time from the start of injection of 0.130 milliseconds.

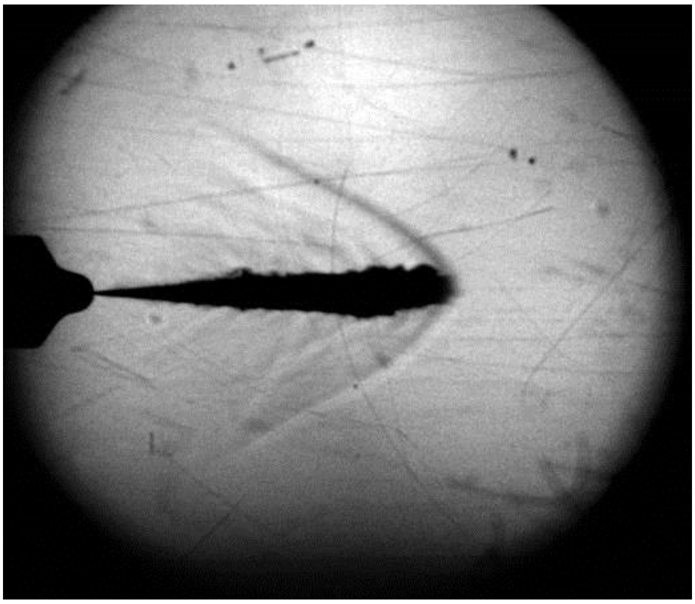

Figure 2. Example of shadowgraphy visualization image for test in sulfur hexafluoride environment.

Later on, the shadowgraphy images are post-processed using a specific tool to determine the spray penetration. This penetration is defined as the maximum distance between the nozzle tip and the spray contour, previously detected using a threshold of 0.5% of the intensity dynamic range, according to the procedure described by Payri et al. [22].

3. Spray visualization results

Figure 3 shows a summary of the detected shockwave evolution in SF_6 from an injection pressure of 130 MPa and a chamber density of 22.6 kg/m^3. In the left hand side of the image, the computed values of the spray tip penetration and spray tip Mach are plotted as a function of the time elapsed after the start of injection. The spray tip Mach is calculated from the time derivative of the spray penetration and the speed of sound in SF_6 at the corresponding thermodynamic conditions, which is estimated at 136.5 m/s.

In the right hand side of the figure, some images from specific moments along the spray evolution are depicted. Initially (up to approximately 0.1 ms, corresponding to a Mach number around 1.5), it is possible to observe the formation of a triangular (also called oblique) shockwave [23] attached to the spray tip, characterized by a certain shockwave semiangle β. This is the situation for the first two depicted images. From that moment onward, the shockwave transitions to a frontal or normal shockwave [23]. This can be clearly seen in the image at 0.11 ms, where the bow-shape tip of the wave appears. Considering all the tests, the transition between both kinds of shockwaves occurs in between one and two time steps of the visualization, corresponding to approximately 0.025 to 0.05 ms. Finally, when the spray tip reaches subsonic conditions, the normal shockwave detaches from the spray tip and continues its evolution at the corresponding speed of sound.

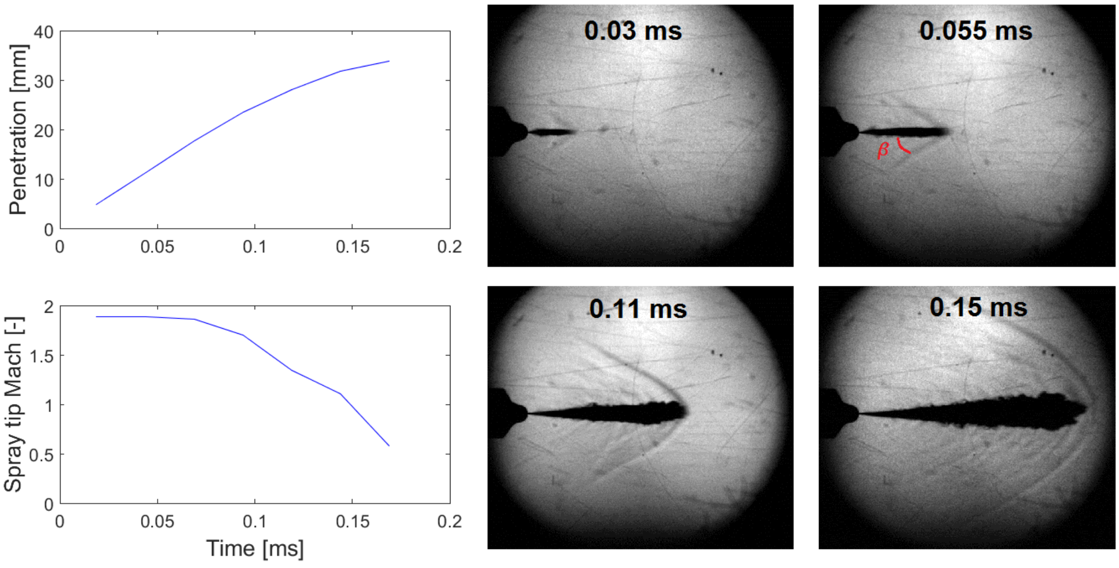

Figure 3. Spray tip penetration, Mach and shockwave analysis for Pi=130 MPa and density 22.6 kg/m^3 from SF_6 tests.

The aforementioned scenario repeats for the rest of the tests performed. Typically, when the spray tip Mach is above 1.5, an oblique shockwave can be detected, while normal or bow-shape shockwave is induced for Mach numbers between 1 and 1.5. Similar transition from triangular to normal shockwaves was identified by Song et al. [17] when passing from high to low spray velocity, but without a clear identification of the Mach threshold for this transition.

Figure 4 shows the spray visualization results for the nozzle outlet diameter of 0.140 mm and chamber density of 22.6 kg/m^3 comparing nitrogen and sulfur hexafluoride. In the left hand side, these results are seen in terms of spray penetration and spray tip Mach for the 50 MPa injection pressure condition. On each curve, the vertical lines represent the measurement standard deviation from all the repetitions taken. As it can be seen, despite the lower speed of sound in SF_6, the spray is always in subsonic regime (no shockwave is generated) and the spray penetration achieved is practically equal for both tests. On the contrary, in the right hand side of the figure the injection pressure is increased to 130 MPa and supersonic conditions are reached for the SF_6 environment. In this case, it can be observed how higher spray penetration compared to nitrogen environment is obtained.

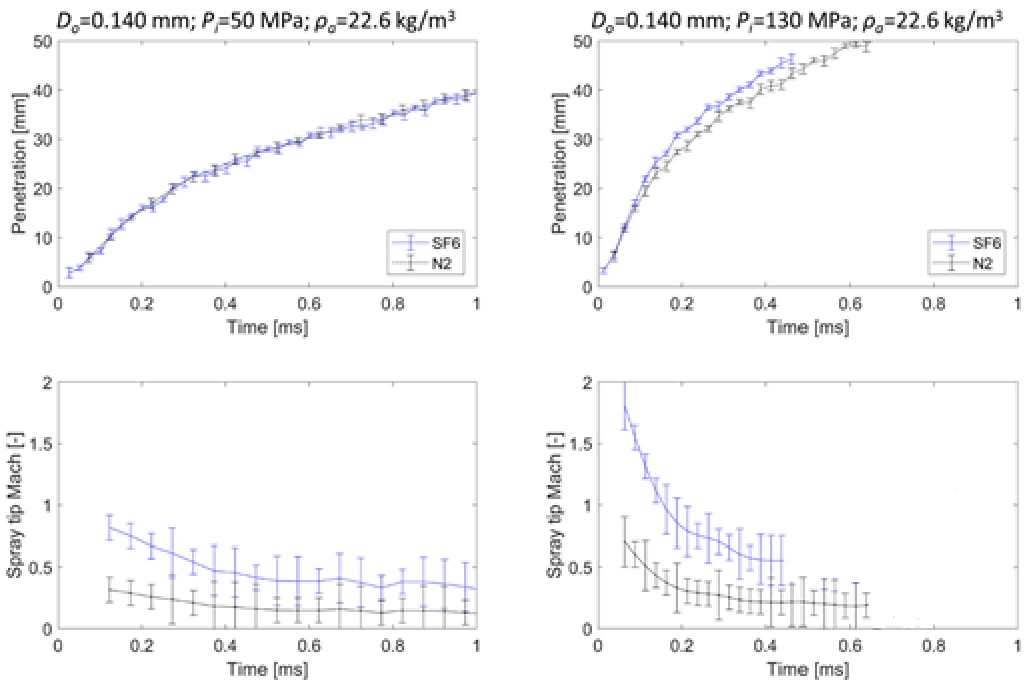

Figure 4. Spray penetration and spray tip Mach results for 0.140 mm nozzle at injection pressures of 50 MPa (left) and 130 MPa (right).

4. Spray penetration correction in supersonic conditions

As stated in section 1, one of the main aspects affecting the spray dynamics is the density ratio between the fuel and the ambient. In the case of the current experiments, this ratio is affected only by the gas density, since fuel composition and temperature are maintained constant. When a shockwave appears during the spray development, a gas density gradient across this shockwave is produced. This density gradient depends mostly on the spray tip Mach number and the kind of shockwave created. In particular, for a frontal or bow-shape wave the following relationship can be used assuming one-dimensional flow [23]:

$$\frac{\rho_{up}}{\rho_{ch}} = \frac{(\gamma+1)M^2}{2+(\gamma-1)M^2} \qquad (1)$$

Where ρ_{up} and ρ_{ch} are the densities upstream the shockwave (i.e. close to the spray tip) and in the rest of the chamber, respectively, γ is the specific heat ratio (equal to 1.0984 for SF_6) and M is the spray tip Mach.

If instead the conditions are such that an oblique shockwave is created, the same relationship applies, but instead of using the experimental spray tip Mach, a corrected Mach, M_n, should be used, which can be calculated as [23]:

$$M_n = M \cdot \sin\beta \qquad (2)$$

where β is the shockwave half angle, as described in Figure 3, which can be extracted from the post-processing images. Nevertheless, it has to be noted that for the conditions evaluated into the experimental campaign, high values of M are typically associated to low values of β, resulting in the fact that the change of density across the shockwave is generally below 5%.

According to equation (1), when supersonic conditions are reached, the density reduces locally in the vicinity of spray. From spray propagation theory, it is known that the density affects penetration with an exponent equal to -0.25 [3,24], so lower density would be translated into a larger spray penetration. Knowing this, it is possible to estimate the supersonic spray penetration at each time step from the subsonic one as:

$$S_{sup}(t) = S_{sup}(t-dt) + \left[S_{sub}(t) - S_{sub}(t-dt)\right]\left(\frac{\rho_{up}(t)}{\rho_{ch}}\right)^{-0.25} \qquad (3)$$

where S_{sup} is the spray penetration at supersonic conditions, S_{sub} is the subsonic one, t is the time elapsed after the start of injection and dt is the time step used to discretize the spray penetration, which depends on the camera velocity for visualization tests. In this expression, the density ratio is calculated at each time step depending on the corresponding spray tip Mach, using expressions (1) and (2) according to the kind of shockwave produced. As a simplification, for the current study it is assumed that for $1<M\leq1.5$, the shockwave is frontal, while for $M>1.5$ it is oblique, which well matches the overall behavior observed in the experiments, arriving to expressions (4) and (5):

$$S_{sup}(t) = S_{sup}(t-dt) + \left[S_{sub}(t) - S_{sub}(t-dt)\right]\left(\frac{(\gamma+1)(M(t)\cdot\sin\beta(t))^2}{2+(\gamma-1)(M(t)\cdot\sin\beta(t))^2}\right)^{-0.25} \quad \text{if } M(t) > 1.5 \tag{4}$$

$$S_{sup}(t) = S_{sup}(t-dt) + \left[S_{sub}(t) - S_{sub}(t-dt)\right]\left(\frac{(\gamma+1)M(t)^2}{2+(\gamma-1)M(t)^2}\right)^{-0.25} \quad \text{if } 1 < M(t) \leq 1.5 \tag{5}$$

Taking into account these considerations, the next step is to evaluate if the differences appreciated into the spray tip penetration between SF_6 and N_2 environment can be explained in terms of this density gradient. This analysis is performed in Figures 5-7. On each of these figures, the following data curves are depicted:

- Experimental spray penetration in N_2 (upper graph, dashed black line) and SF_6 (upper graph, continuous blue line). The lines represent the average values, while the error bars are the experimental uncertainty estimated from the standard deviation along the eight repetitions.
- Theoretical spray tip Mach (bottom graph). It represents the Mach that the spray tip would reach considering the tip velocity obtained from the N_2 measurements penetration gradient, but considering the speed of sound characteristic of SF_6.
- Corrected (or supersonic) N_2 penetration curve (upper graph, dashed red line), calculated using equations (4) and (5). The aim of this correction is to see if the methodology described previously can help to predict the supersonic penetration from the subsonic one.

The first results presented in Figure 5 correspond to a subsonic case, reached with a low injection pressure and a high ambient density. As it could be expected, when the flow regime is subsonic, no density gradient appears, and all three curves are practically equal.

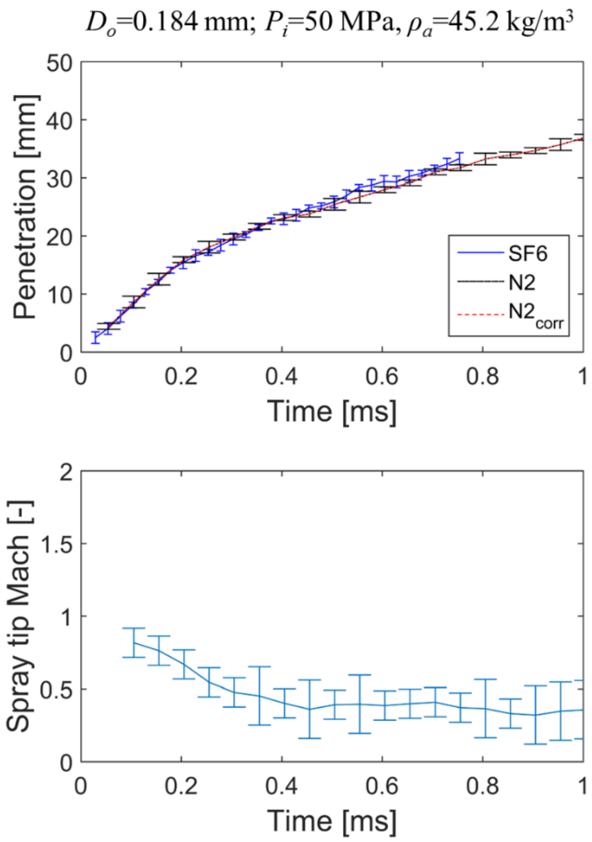

Figure 5. Spray penetration evaluation for D_o=0.184 mm; P_i=50 MPa, ρ_a=45.2 kg/m^3.

Figure 6 represents a case where supersonic conditions are reached, mostly due to the increase of injection pressure. Nevertheless, the maximum *M* is around 1.5, which according to the previous analysis would imply that only normal shockwaves would be produced. From the experimental values, it can be clearly seen how the spray penetration is larger for the SF_6 tests, as already anticipated from the density ratio expressions. Once the correction is applied to the N_2 results, both curves present again a very good agreement. This can be seen as a confirmation that the most significant differences observed in terms of spray penetration are directly related to the density gradient produced by the shockwave.

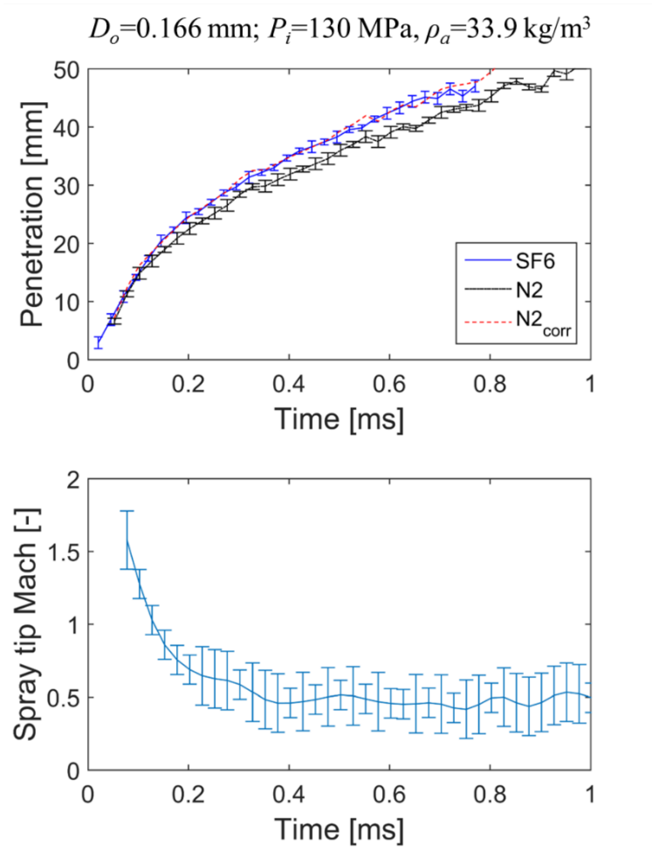

Figure 6. Spray penetration evaluation for D_o=0.166 mm; P_i=130 MPa, ρ_a=33.9 kg/m^3.

Finally, Figure 7 shows a case with a lower ambient density and a larger nozzle diameter, which produce faster spray penetration and higher Mach. In this case, it can be seen how both experimental curves are very similar up to ~0.1 ms after the start of injection. This behavior is quite well reproduced also by the corrected spray penetration, since oblique shockwaves with lower density ratios would be predicted. Once the spray tip velocity reduces and the shockwave transitions from oblique to normal, the two experimental curves detach, behavior that is also well predicted according to the transition between equations (4) and (5).

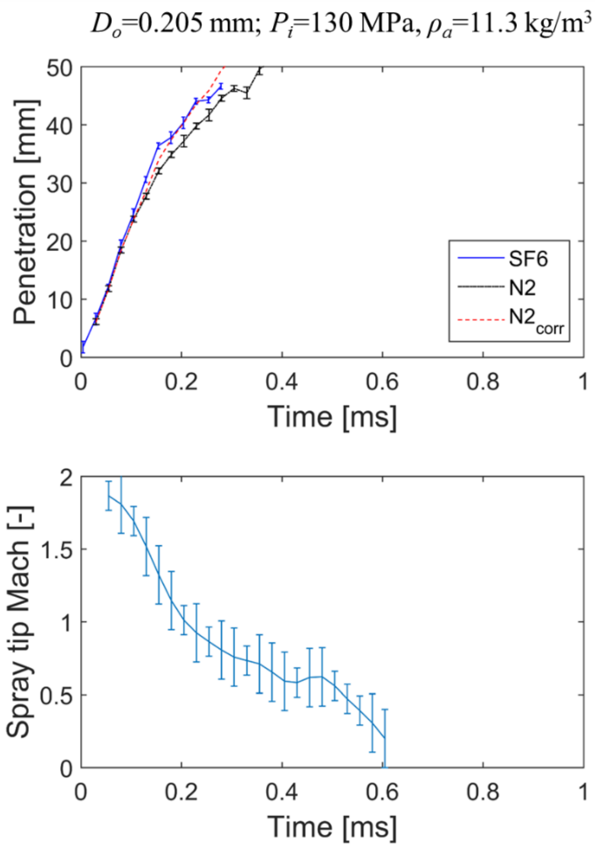

Figure 7. Spray penetration evaluation for D_o=0.205 mm; P_i=130 MPa, ρ_a=11.3 kg/m^3

While in the current study the subsonic penetration has been directly taken from the N_2 experiments, the advantage of this methodology is that there are well established models and experimental correlations that can be used to accurately estimate this penetration. Nevertheless, these predictions could significantly underestimate the spray penetration if supersonic conditions are reached. According to the results just discussed, this underprediction can be easily corrected by calculating the spray tip Mach and the corresponding density ratio, as previously described.

Figure 8 shows the values of spray tip Mach and the subsequent spray penetration correcting factor that could be expected in engine environment (with air as working gas) for the fuel injector with 0.119 mm diameter, which is the most representative of a light-duty application. This spray tip Mach is computed as a function of the combustion chamber temperature, which affects the speed of sound, and the fuel injection pressure, controlling the spray tip penetration. The temperature is changed in a range from 300 K (approximately room temperature, as the conditions tested in the current work) to 1000K. In the case of the injection pressure, the range has been extended up to 350 MPa, which is seen as a reasonable future capability for diesel fuel injection systems considering that there are already production samples operating at 300 MPa. The spray penetration law used to obtain the spray tip Mach is obtained using the model proposed by Desantes et al. [25], which derives the penetration from the spray momentum. This spray momentum has been estimated as a function of the fuel injection pressure using the following expression:

$$\dot{M}_o = \rho_f A_{eff} u_{eff}^2 = \rho_f C_a A_o C_v^2 u_{th}^2 = 2 C_a A_o C_v^2 (P_i - P_{ch}) \qquad (6)$$

Where $\dot{M}_o$ is the spray momentum at the nozzle outlet, ρ_f is the fuel density, A_{eff} is the nozzle effective outlet area, u_{eff} is the nozzle effective outlet velocity, C_a and C_v are the nozzle area and velocity coefficients, A_o is the nozzle geometrical outlet area, u_{th} is the nozzle outlet velocity according to Bernoulli's equation and P_i and P_{ch} are the injection and chamber pressure, respectively [26]. Since no experimental information regarding area and velocity coefficients is available for most of the injection pressure range evaluated, since it is out of the fuel injector capabilities, constant values of 0.98 and 0.9 have been used for this estimation. Regarding the chamber pressure, also a constant value of 5 MPa has been selected as a simplification. Finally, a constant spray cone opening angle of 20º was also considered to compute the spray tip penetration as a simplification.

Looking at this figure, it can be seen how up to 200 MPa injection pressure the conditions are always subsonic, so no correction is necessary. On the contrary, for higher injection pressures supersonic conditions appear, and for 350 MPa spray penetration would always be impacted regardless the chamber temperature used. The impact on spray penetration can be as high as 16% for the most critical conditions evaluated.

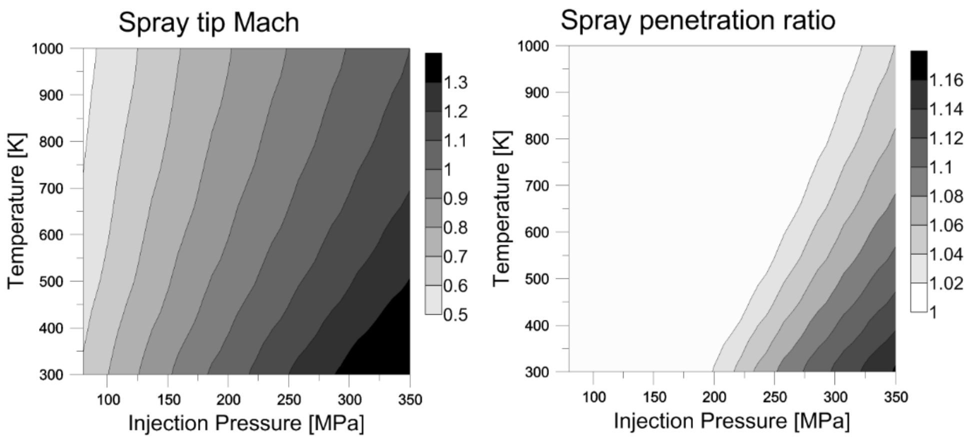

Figure 8. Analysis of potential spray tip Mach and spray penetration correction in engine environment vs. temperature and injection pressure.

However, it has to be noted that the information in Figure 8 has two main simplifications with respect to real engine-like operation. First, this calculation assumes constant thermodynamic conditions (thus density). In reality, pressure and temperature in the combustion chamber vary as a consequence of the piston compression. Nevertheless, the use of multiple injections with short durations in current diesel engines make that the variation of these thermodynamic conditions during the spray propagation time is very small, so the impact should be negligible, and the only uncertainty in this regard for engine operation would be the determination of the combustion chamber temperature needed to evaluate the density. The most significant simplification instead comes from the fact that the so called free spray assumption is taken. This means that spray propagation is not affected by the combustion chamber air motion nor by the interaction with the combustion chamber walls. While for heavy duty applications, which are characterized by large bores and quiescent combustion systems (i.e. with low swirl motion) this assumption may be acceptable, the effects of spray-wall interactions and air motion should be considered for other applications.

5. Conclusions and future works.

In the current study, an investigation of diesel spray penetration characteristics on supersonic conditions has been performed. These supersonic conditions have been obtained by injecting into a sulfur hexafluoride environment, characterized by a lower speed of sound. The following conclusions have been drawn:

- From the SF_6 visualization tests, two different kinds of shockwaves have been detected: oblique, when the spray tip velocity is high, and normal, for lower values. The transition between both regimes can be found around a spray tip Mach approximately equal to 1.5.
- Spray tip penetration is generally higher in SF_6 environment than in N_2 once supersonic conditions are reached. This higher penetration is associated to the density ratio appearing across the shockwave, producing a lower density than anticipated in the spray tip vicinity.
- A methodology based on one-dimensional flow approximation for supersonic shockwaves and the typical exponent for the chamber density in spray penetration correlations is proposed to extrapolate supersonic spray penetration from subsonic values, showing good agreement with the experimental data.

From the current study, three main paths for future works arise. The first would be to perform the supersonic spray characterization at ultra-high injection pressure (over 200 MPa) in order to confirm that the methodology proposed is capable to accurately predict these conditions. The second proposal for future work would be to explore close-coupled multiple injections. In this case, the second injection would encounter an environment partially filled with vaporized diesel fuel, which would reduce the local speed of sound and potentially enhance the supersonic conditions at the same injection velocity. Finally, another potential field of interest would be to extend this work to an optical engine, where the effects of air motion and spray-wall interactions can be accounted for.

NOMENCLATURE

A_{eff}	Nozzle outlet effective area.
A_o	Nozzle outlet area.
C_a	Nozzle area coefficient.
C_v	Nozzle velocity coefficient.
D_o	Injector nozzle outlet diameter.
dt	Time step for the visualization tests.
M	Spray tip Mach.
$\dot{M}_o$	Momentum flux at the nozzle outlet.
P_{ch}	Discharge chamber pressure.
P_i	Injection pressure.
S	Spray tip penetration.
S_{sub}	Spray tip penetration in subsonic conditions.
S_{sup}	Spray tip penetration in supersonic conditions.
t	Time elapsed after the start of injection.
u_{eff}	Nozzle outlet effective velocity.
u_{th}	Nozzle outlet theoretical velocity according to Bernoulli's equation.

Greek symbols

ρ_f	Fuel density.
ρ_a	Air density.
γ	Specific heat ratio.
β	Oblique shockwave angle
ρ_{ch}	Discharge chamber density far from the shockwave.
ρ_{up}	Discharge chamber density upstream the shockwave.

REFERENCES

[1] Naber JD, Siebers DL. Effect of gas density and vaporization on penetration and dispersion of Diesel sprays. SAE Trans J Engines 1996;105:82--111. doi:10.4271/960034.

[2] Sazhin SS, Feng G, Heikal MR. A model for fuel spray penetration. Fuel 2001;80:2171–80. doi:10.1016/S0016-2361(01)00098-9.

[3] Wan Y, Peters N. Scaling of spray penetration with evaporation. At Sprays 1999;9:111–32.

[4] Payri R, Salvador FJ, Gimeno J, Novella R. Flow regime effects on non-cavitating injection nozzles over spray behavior. Int J Heat Fluid Flow 2011;32:273–84. doi:10.1016/j.ijheatfluidflow.2010.10.0.

[5] Sazhin S, Crua C, Kennaird D, Heikal M. The initial stage of fuel spray penetration☆. Fuel 2003;82:875–85. doi:10.1016/S0016-2361(02)00405-2.

[6] Payri R, Salvador FJ, Gimeno J, De La Morena J. Macroscopic behavior of diesel sprays in the near-nozzle field. SAE Tech. Pap., 2008. doi:10.4271/2008-01-0929.

[7] Mohan B, Yang W, Chou SK. Fuel injection strategies for performance improvement and emissions reduction in compression ignition engines—A review. Renew Sustain Energy Rev 2013;28:664–76. doi:10.1016/j.rser.2013.08.051.

[8] Choi W, Choi B-C. Estimation of the air entrainment characteristics of a transient high-pressure diesel spray. Proc Inst Mech Eng Part D J Automob Eng 2005;219:1025–36. doi:10.1243/095440705X34630.

[9] Braun T, Rabl H-P, Mayer W. Emission Reduction Potential by Means of High Boost and Injection Pressure at Low- and Mid- Load for a Common Rail Diesel Engine under High EGR Rates. SAE Int 2013. doi:10.4271/2013-01-2541.

[10] Wang ZG, Wu L, Li Q, Li C. Experimental investigation on structures and velocity of liquid jets in a supersonic crossflow. Appl Phys Lett 2014;105:1–5. doi:10.1063/1.4893008.

[11] Tao F, Bergstrand P. Effect of Ultra-High Injection Pressure on Diesel Ignition and Flame under High-Boost Conditions. SAE Tech Pap 2008-01-1603 2008. doi:10.4271/2008-01-1603.

[12] Kostas J, Honnery D, Soria J, Kastengren a., Liu Z, Powell CF, et al. Effect of nozzle transients and compressibility on the penetration of fuel sprays. Appl Phys Lett 2009;95:2009–11. doi:10.1063/1.3182821.

[13] Hillamo H, Sarjovaara T, Kaario O, Vuorinen V, Larmi M. Diesel spray visualization and shockwaves. At Sprays 2010;20 (3):177–89.

[14] Jia TM, Li GX, Yu YS, Xu YJ. Propagation characteristics of induced shock waves generated by diesel spray under ultra-high injection pressure. Fuel 2016;180:521–8. doi:10.1016/j.fuel.2016.04.009.

[15] Jia TM, Li GX, Yu YS, Xu YJ. Effects of ultra-high injection pressure on penetration characteristics of diesel spray and a two-mode leading edge shock wave. Exp Therm Fluid Sci 2016;79:126–33. doi:10.1016/j.expthermflusci.2016.07.006.

[16] Wang Y, Yu YS, Li GX, Jia TM. Experimental investigation on the characteristics of supersonic fuel spray and configurations of induced shock waves. Sci Rep 2017;7:1–8. doi:10.1038/srep39685.

[17] Song E, Li Y, Dong Q, Fan L, Yao C, Yang L. Experimental research on the effect of shock wave on the evolution of high-pressure diesel spray. Exp Therm Fluid Sci 2018;93:235–41. doi:10.1016/j.expthermflusci.2018.01.004.

[18] Payri R, Salvador FJ, De la Morena J, Pagano V. Experimental investigation of the effect of orifices inclination angle in multihole diesel injector nozzles. Part 2 – Spray characteristics. Fuel 2018;213:215–21. doi:10.1016/j.fuel.2017.07.076.

[19] Salvador FJ, Carreres M, De la Morena J, Martínez-Miracle E. Computational assessment of temperature variations through calibrated orifices subjected to high pressure drops:

Application to diesel injection nozzles. Energy Convers Manag 2018;171:438–51. doi:10.1016/j.enconman.2018.05.102.

[20] Payri R, Salvador FJ, Garcia A, Gil A. Combination of visualization techniques for the analysis of evaporating diesel sprays. Energy & Fuels 2012;26:5481–90. doi:10.1021/ef3008823.

[21] Payri R, Gimeno J, De la Morena J, Battiston PA, Wadhwa A, Straub R. Study of new prototype pintle injectors for diesel engine. Energy Convers Manag 2016;122:419–27. doi:10.1016/j.enconman.2016.06.003.

[22] Payri R, Gimeno J, Viera JP, Plazas AH. Needle lift profile influence on the vapor phase penetration for a prototype diesel direct acting piezoelectric injector. Fuel 2013;113:257–65. doi:10.1016/j.fuel.2013.05.057.

[23] Anderson Jr. JD. Modern Compressible Flow: with historical perspective. New York, NY (USA): McGraw-Hill Education; 1982.

[24] Dhar A, Tauzia X, Maiboom A. Phenomenological models for prediction of spray penetration and mixture properties for different injection profiles. Fuel 2016;171:136–42. doi:10.1016/j.fuel.2015.12.022.

[25] Desantes JM, Payri R, Salvador FJ, Gil A. Development and validation of a theoretical model for diesel spray penetration. Fuel 2006;85:910–7.

[26] Bermúdez, V., Payri, R., Salvador, FJ, Plazas, A. Study of the influence of nozzle seat type on injection rate and spray behavior, Proceedings of the institution of mechanical engineers Part D- Journal of automobile engineering; 2005; 219, 677-689.